

D.V.Skobel'tsyn Institute of Nuclear Physics  
M.V.Lomonosov Moscow State University

INP MSU Preprint 99-42/600

Yu.A. Golubkov<sup>a)</sup>, M.Yu. Khlopov<sup>b)</sup>

## Diffuse Gamma Flux from Antiproton Annihilation in Our Galaxy

<sup>a)</sup>*Institute of Nuclear Physics, Moscow State University, Vorobjevy Gory,  
119899, Moscow, Russia,*

<sup>b)</sup>*Institute of Applied Mathematics, Miusskaya Pl.4, 125047, Moscow, Russia,*

Moscow 1999

Yu.A. Golubkov<sup>a)</sup>, M.Yu. Khlopov<sup>b)</sup>

<sup>a)</sup>e-mail: golubkov@npi.msu.su

<sup>b)</sup>e-mail: mkhlopov@orc.ru

Preprint of Institute of Nuclear Physics 99—42/600

## Diffuse Gamma Flux from Antiproton Annihilation in our Galaxy

### Abstract

The all-sky survey in high-energy gamma rays ( $E > 30$  MeV) carried out by the Energetic Gamma Ray Experiment Telescope (EGRET) aboard the Compton Gamma-Ray Observatory provides a unique opportunity to examine in detail the diffuse gamma-ray emission. The observed diffuse emission has a Galactic component arising from cosmic-ray interactions with the local interstellar gas and radiation as well as an almost uniformly distributed component that is generally believed to originate outside the Galaxy. The results of the observations have been interpreted as the extragalactic high-energy gamma-ray emission arising primarily from unresolved gamma-ray-emitting blazars.

Here we consider another possible origin of the diffuse gamma-ray flux, namely, as originating from the annihilation of the antiprotons with the interstellar medium.

# 1 The annihilation cross sections

The existing theoretical models based mainly on the partonic picture of the hadronic interactions are definitely invalid for  $\bar{p}p$  annihilation at low energies. Due to this fact we used experimental data as for evaluation of the annihilation cross section as well as for the simulation of the final state and secondaries distribution.

The annihilation cross section is the difference between total and inelastic ones  $\sigma_{ann} \approx \sigma_{tot} - \sigma_{el}$ . As it follows from data the dependence  $\sigma_{ann} \sim v^{-1}$  is valid already for laboratory antiproton momenta  $p_{lab} \leq 1000$  MeV/c. Thus, at  $P_{lab} \geq 300$  MeV/c we used data from [1] for the total and elastic cross sections and at momenta lesser than 300 MeV we used the dependence

$$\sigma_{ann}(P < 300 \text{ MeV}) = \sigma_0 C(v^*)/v^* \text{ for annihilation cross section,}$$

and

$$\sigma_{el} = \text{const for elastic cross section}$$

The additional Coulomb factor  $C(v^*)$  gives large increase for the annihilation cross section at small velocities of the antiproton and is defined by the expression [2]:

$$C(v^*) = \frac{2\pi v_c/v^*}{1 - \exp(-2\pi v_c/v^*)},$$

where,  $v_c = \alpha c$ , with  $\alpha$  being the fine structure constant and  $c$  being the speed of light and  $v^*$  is the velocity of the antiproton in the center-of-mass  $\bar{p}p$  system.

We used the experimental data on the  $\bar{p}p$  annihilation cross section [3, 4] to normalize the  $1/v$  behaviour and the Coulomb factor, choosing:

$$\sigma_0 = \sigma_{ann}^{exp}(P = 300 \text{ MeV}) \approx 160 \text{ mb.}$$

---

<sup>1</sup>Invited talk at the IV Int. Conf. "Cosmion-99", Moscow, October 17-24, 1999

## 2 Gamma flux

We used the experimental data [5] on the  $\bar{p}p$  annihilation at rest to simulate the distribution of the final state particles, see Table.

Table. Relative probabilities of  $\bar{p}p$  annihilation channels.

Channel	Rel. prob., %	Channel	Rel. prob., %
$\pi^+\pi^-\pi^0$	3.70	$2\pi^+2\pi^-\eta$	0.60
$\rho^-\pi^+$	1.35	$\pi^0\rho^0$	1.40
$\rho^+\pi^-$	1.35	$\eta\rho^0$	0.22
$\pi^+\pi^-2\pi^0$	9.30	$4.99\pi^0$	3.20
$\pi^+\pi^-3\pi^0$	23.30	$\pi^+\pi^-$	0.40
$\pi^+\pi^-4\pi^0$	2.80	$2\pi^+2\pi^-$	6.90
$\omega\pi^+\pi^-$	3.80	$3\pi^+3\pi^-$	2.10
$\rho^0\pi^0\pi^+\pi^-$	7.30	$K\bar{K}0.95\pi^0$	6.82
$\rho^+\pi^-\pi^+\pi^-$	3.20	$\pi^0\eta'$	0.30
$\rho^-\pi^+\pi^+\pi^-$	3.20	$\pi^0\omega$	3.45
$2\pi^+2\pi^-2\pi^0$	16.60	$\pi^0\eta$	0.84
$2\pi^+2\pi^-3\pi^0$	4.20	$\pi^0\gamma$	0.015
$3\pi^+3\pi^-\pi^0$	1.30	$\pi^0\pi^0$	0.06
$\pi^+\pi^-\eta$	1.20		

In practice, the approximation of the annihilation at rest is valid with very good accuracy up to laboratory momentum of the incoming antiprotons about 0.5 GeV because at this laboratory momentum the kinetic energy of the antiproton is still order of magnitude lesser than the twice antiproton mass. The average number of  $\gamma$ 's per annihilation is

$$N_\gamma = 3.93 \pm 0.24.$$

The simulation of the distributions of final state particles has been performed according to phase space in the center-of-mass of the  $\bar{p}p$  system. After that PYTHIA 6.127 package [6] has been used to perform the decays of all unstable and quasi-stable particles.

We used the spherical model for halo and parametrized the density distribution of interstellar hydrogen gas along the  $z$  direction (to North Pole) as:

$$n_H(z) = n_H^{halo} + \frac{n_H^{disc}}{1 + (z/D)^2},$$

where  $n_H^{halo} = 10^{-2} \text{ cm}^{-3}$  is the hydrogen number density in the halo,  $n_H^{disc} = 1 \text{ cm}^{-3}$  is the hydrogen number density in the disc and  $D = 100 \text{ pc}$  is the half-width of the gaseous disc. The number of gammas arriving from the given direction is defined by the well known expression:

$$J_\gamma(E) = \int_0^L dl \psi(E, r, z).$$

Here  $\psi(E)$  is the density of gamma source along the observation direction  $l$  in suggestion of the isotropic distribution of the gamma source. The integration must be performed up to the edge of the halo  $L = -\alpha_x R_\odot + \sqrt{R_{halo}^2 - R_\odot^2 (1 - \alpha_x^2)}$  with  $\alpha_x$  being the cosine of the line-of-sight to the  $x$  axis.

The flux of the antiprotons has been chosen similar to the standard proton flux:

$$J_{\bar{p}}(E_{kin}) = N_{tot} \beta \left( \frac{1 \text{ GeV}}{E_{kin}} \right)^{2.7},$$

where  $\beta = p/E$  is the dimensionless antiproton velocity. The minimal kinetic energy of the antiprotons has been chosen equal to the velocity dispersion in the Galaxy,  $v_{min} \approx 300 \text{ km/s}$ , i.e.,

$$E_{kin}^{min} \approx 500 \text{ eV}.$$

Fig.1(a,b) demonstrates the resulting differential gamma distribution in the Galactic North Pole direction in comparison with EGRET data [7] in the range  $10 \leq E_\gamma \leq 1000 \text{ MeV}$ . The peak of  $\pi^0$  decay is clearly seen both in calculations as well as in experimental distributions. Fig.1(c) shows the charged multiplicity distribution in the annihilation model described above. Experimental points have been taken from [8, 9].

At this choice the necessary integral number density of the antiprotons  $N_{tot}$  is:

$$N_{tot} = \int_{E_{min}}^{\infty} \frac{dN_{\bar{p}}(E)}{dE_{kin}} \sim 10^{-13} \text{ cm}^{-3}.$$

Note here, that within reasonable variation of the index of the antiproton flux the integral number of the antiprotons does not varies significantly. This is due to the fact that the main contribution comes from the  $\bar{p}p$  annihilation at the lowest velocity of the antiprotons. If we choose the minimal velocity of antiprotons according the velocity of the stellar wind,  $v_{wind} \approx 1000 \text{ km/s}$ , the necessary antiproton number density must be increased by order of magnitude and is  $N_{tot} \sim 10^{-12} \text{ cm}^{-3}$ . This number also does not contradict to any theoretical or experimental limits on relative amount of the antimatter.

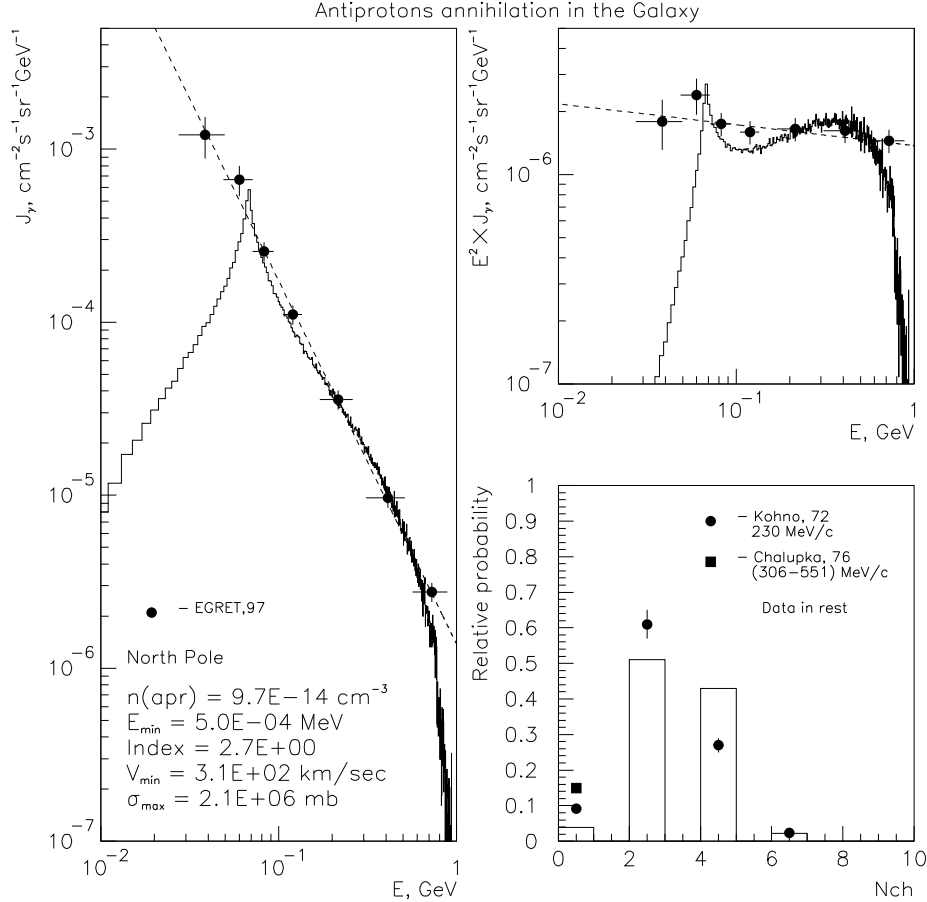


Figure 1: Comparison of the calculated differential fluxes of  $\gamma$  quanta from  $\bar{p}p$  annihilation with experimental data *EGRET* [7] on diffuse gamma background (a,b). There is also shown the charged multiplicity distribution in the annihilation model described in the text (c).

### 3 Discussion. Antimatter Globular Cluster

We considered the stationary case, provided by the presence of a permanent source of the antimatter. Assume [10] that antimatter stars in the Galaxy form globular cluster, moving along elliptical orbit in the halo. In the first approximation the integral effect we study depends on the total mass of the antimatter stars in the Galaxy and it does not depend on the amount of globular clusters. The main contribution into galactic gamma radiation comes from the antimatter lost by the cluster and spread over the Galaxy.

There are two main mechanisms of antimatter loss by the cluster. The first one is the stationary mass loss by antimatter stars in the form of stellar wind. The second mechanism is the antimatter Supernova explosions. In both cases the antimatter is spread over the Galaxy in the form of positrons and antinuclei. Due to traveling in the halo magnetic fields the emitted antiprotons fill the whole halo and one can consider their number density to be constant over the halo.

To evaluate the confinement time for the antiprotons in the Galaxy we used the

results of the "two-zone" leaky box model [11]. As the confinement time enters as a common factor in the predicted  $\bar{p}p$  ratio [11], we can find the necessary factor, performing the fit of the normalization to the experimental data. We removed from the fit two the most left points, strongly affected by the heliosphere [12]. Solid curve in Fig.2(a) presents the LBM predictions for the  $\bar{p}p$  ratio, multiplied by the fitted factor  $K = 2.58$ , which factor increases the confinement time for slow antiprotons in the Galaxy up to  $2 \cdot 10^8$  years. Dashed curve is the phenomenological fit in the form  $R(E) = a E^{b+c \lg E}$ . Experimental points have been taken from [13] where references on the data can be found.

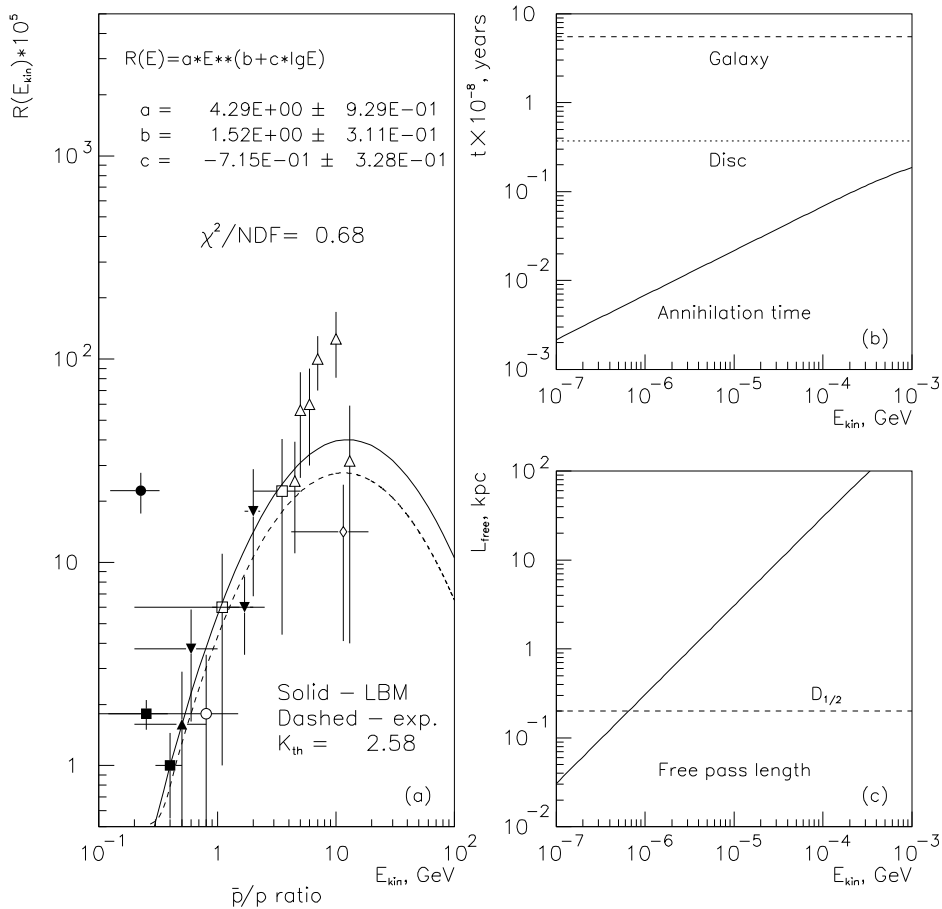


Figure 2: (a) Fit of the  $\bar{p}p$  ratio to experimental data. Solid line shows predictions of the two-zone leaky box model, increased by factor  $K \approx 2.6$ . Dashed curve is the phenomenological fit, described in the text. (b) The comparison of the antiprotons annihilation time in the disc (solid) with the predicted LBM confinement time from Galaxy (dashed) and from disc (dot-dashed). (c) The free pass length of antiprotons in the disc. Dashed line shows the half-width of the disc.

Fig.2 shows also the time of life of the antiprotons in the disc (b) and the free pass length of the antiprotons in the disc (c) versus antiproton kinetic energy. The correspondent curves for halo can be easily obtained if one reduces the hydrogen number density by two-three orders of magnitude according to  $H$  number density in the halo. Note here that the presented in Fig.2 confinement time for very

slow antiprotons has been extrapolated to small kinetic energies, suggesting that  $t_{esc}(E_{kin} < 0.1 GeV) \approx const = t_{esc}(E_{kin} = 0.1 GeV)$  and is, in fact, the lower limit for the confinement time.

From Fig.2(b) we can conclude that confinement time for low-energy antiprotons in the halo and in the gaseous disc is much greater than their life time with respect to the annihilation. Therefore we can consider the picture as a stationary one. From Fig.2(c) we see, that free pass length of the slowest antiprotons is lesser than the half-width of the disc and we can observe the products of the annihilation only but not the original antiprotons. The detailed analysis of the antimatter annihilation mechanism for Galactic diffuse gamma flux in the terms of antimatter globular cluster and the estimation of the total amount of antimatter stars and the expected antihelium flux for this case will be considered in the successive paper.

*Acknowledgements.* The authors acknowledge the COSMION Seminar participants for useful discussions. The work was partially supported by Section "Cosmoparticle Physics" of State Scientific Technical Programme "Astronomy. Fundamental Space Research" and performed in the framework of COSMION-ETHZ and AMS-EPICOS collaborations of ASTRODAMUS project.

## References

- [1] Review of Particle Physics, *Phys. Rev. D*, 1996, ,vol. 54, p. 191.
- [2] L.D.Landau and E.M.Lifshits. *Quantum Mechanics*. Fizmatgiz, Moscow, 1963.
- [3] *Phys. Lett. B*, 1996, v.369, p.77.
- [4] *Z. Phys. A*, 1990, v.335, p.217.
- [5] G.Backenstoss et al. *Nucl. Phys. B*, 1983, v.228, p.424.
- [6] T. Sjostrand, *Computer Physics Commun.*, 1982, v.82, p.74.
- [7] P.Sreekumar et al. *astro-ph/9709257*.
- [8] H.Kohno et al. *Nucl. Phys. B*, 1972, v.41, p.485.
- [9] V.Chaloupka et al. *Phys. Lett. B*, 1976, v.61, p.487.
- [10] M.Yu.Khlopov, *Gravitation and Cosmology*, 1998, vol. 4, p. 1.
- [11] P.Chardonnet, G.Mignola, P.Salati and R.Taillet, *Preprint CERN-TH/96-114, ENSLAPP-A-550/96, astro-ph/9606174*.
- [12] S.H.Geer and D.C.Kennedy, *Preprint FERMILAB-PUB-98/265-A, UF-IFT-HEP-98-13, astro-ph/9809101*.
- [13] Yu.A.Golubkov and R.V.Konoplich, *Phys.Atom.Nucl.*, **61** (1998) 602; *hep-ph/9704314*.